Mathematical Biosciences and Engineering

http://www.aimspress.com/journal/MBE

MBE, 16(6): 7098–7111.
DOI: 10.3934/mbe.2019356
Received: 01 April 2019
Accepted: 17 July 2019
Published: 05 August 2019

Research article

A mathematical model of chromosome recombination-induced drug resistance in cancer therapy

Hongli Yang[1] **and Jinzhi Lei**[2,*]

[1] School of Mathematical Sciences, Inner Mongolia University, Hohhot 010021,China

[2] Zhou Pei-Yuan Center for Applied Mathematics, MOE Key Laboratory of Bioinformatics, Tsinghua University, Beijing 100084, China

* **Correspondence:** Email: jzlei@tsinghua.edu.cn; Tel: +86-10-62795156.

Abstract: Cytotoxic chemotherapeutics are common treatment methods of many cancers, and patients are often dosed at maximum tolerated dose (MTD), which is trying to eliminate cancer cells as much as possible. However, highly doses chemotherapy may induce unexpected gene mutations or DNA recombinations, which in turn result in unpredictable outcomes and drug resistance. In this study, we focus on the occurrence of DNA recombinations, and present a mathematical model for the influence of genomic disorder due to chemotherapy, and investigate how it may lead to drug resistance. We show that there is an optimal dose so that the tumor cells number is minimum at the steady state, which suggests the existence of an optimal dose of chemotherapy below the MTD. Model simulations show that when the dose is either low or high, the tumor cancer cells number may maintain a higher level steady state, or even sustained oscillations when the dose is too high, which are clinically inappropriate. Our results provide a theoretical study on the dose control of chemotherapy in cancer therapy.

Keywords: delay differential equation; genomic disorder; non-clonal chromosome aberrations; chemotherapy; drug resistance

1. Introduction

Cancer is a group of diseases involving abnormal cell growth [1, 2]. Currently, despite great progresses of many newly developed therapeutic methods [3–5], chemotherapy is still a common treatment method for many cancers. Patients are often administrated with high-dose of cytotoxic chemotherapeutics trying to eliminate tumor cells as much as possible [6–11]. Nevertheless, it is difficult to determine the proper dosage of chemotherapy, low dosage is ineffective in killing tumor cells, whereas excessive dosage may result in additional toxicity that is intolerable to patients [6].

Clinically, patients are often dosed at maximum or near maximum tolerated dose, which is carefully determined in phase I studies [7, 12]. However, high level doses often induce series side-effects, increasing the chemotherapy dose (also the treatment cost) would not yield the decreasing of the recurrence rate [13, 14]. The recurrent tumors often show drug resistance, which is a major cause of treatment failure in chemotherapeutic drugs [15–17].

Drug resistance has been a major challenge in cancer therapy. The mechanisms of drug resistance are complex, and many reasons are involved, including cellular plasticity [18], heterogenous tumor cells [19], or therapy induced gene mutations [20, 21]. In this study, we focus on a mechanism of drug resistance due to chemotherapy-induced genome instability. Chemotherapy agents are cytotoxic by means of interfering with cell division in a way of damaging or stressing cells, and leading to cell death through apoptosis. During the early stage of apoptosis, apoptotic chromosome fragmentation (C-Frag) are produced through the cleavage by caspase-3 activated DNase (CAD) [22]. Nevertheless, C-Frag does not always result in cell death, sometimes the chromosome fragments can randomly rejoin to form genome chaos so that the cells survive from crisis [23, 24]. These survived cells carry non-clonal chromosome aberrations (NCCAs), the major form of genome variation and the key index of genome instability in cancer cells [25–28]. It was proposed that such genome instability induced by chemotherapy is a source of drug resistance in cancer therapy [26, 27]; quantitative control of drug dosages is important for the long-term clinical effects.

Mathematical modelling approaches have been widely used in cancer research from different aspects [2, 29]. A variety of models have been established to study the mechanisms of drug resistance after chemotherapy [30–34]. However, there are rare quantitative studies on how tumor cells population change in response to chemotherapy and drug resistance due to therapy-induced chromosome recombination. The roles of NCCAs in tumor recurrence is still controversial [35].

In this study, we intend to investigate how NCCAs may affect tumor growth, and present a mathematical model for chromosome recombination-induced drug resistance in cancer therapy. The model extends the previously well studied G0 cell cycle model [36–39], and includes cell survival from C-Frag [23, 24]. We mainly study cell population responses to various doses of chemotherapy, and show that there is an optimal dose (within the maximum tolerated dose) so that the steady state tumor cell number is relative low after chemotherapy. Moreover, the model implies that persistent extreme high dose therapy may induce oscillations in cell number, which is clinically inappropriate and should be avoided.

2. Model formulation

In this study, we model the process of tumor growth through formulations of stem cell regeneration. Here, we mainly consider chemotherapy for leukemia, and mathematical models of hematopoiesis are referred in our modeling. We refer the classical G0 cell cycle model that has long been studied in literatures [40–42] (Figure. 1(a)). In the model, leukemia stem cells are classified as either resting or proliferative phase cells. Resting phase cells (Q, cells/kg) either enter the proliferative phase at a rate β (day^{-1}), or be removed from the pool of resting phase due to differentiation, senescence, or death, at a rate κ (day^{-1}). The cells at the proliferative phase undergo apoptosis in a rate μ (day^{-1}), and the duration of the proliferative phase is τ (days), each survived cell divides into two daughter cells through mitosis at the end of the proliferative phase. These processes can be described by a delay differential

equation model [36–39]:

$$\frac{dQ}{dt} = -(\beta(Q) + \kappa)Q + 2e^{-\mu\tau}\beta(Q_\tau)Q_\tau. \tag{2.1}$$

Here, the subscript means the time delay, *i.e.*, $Q_\tau = Q(t - \tau)$. The equation (2.1) has been widely applied in the study of hematopoietic stem cell regeneration dynamics and blood disease [43–46], as well as the hematopoietic responses to chemotherapy [47, 48].

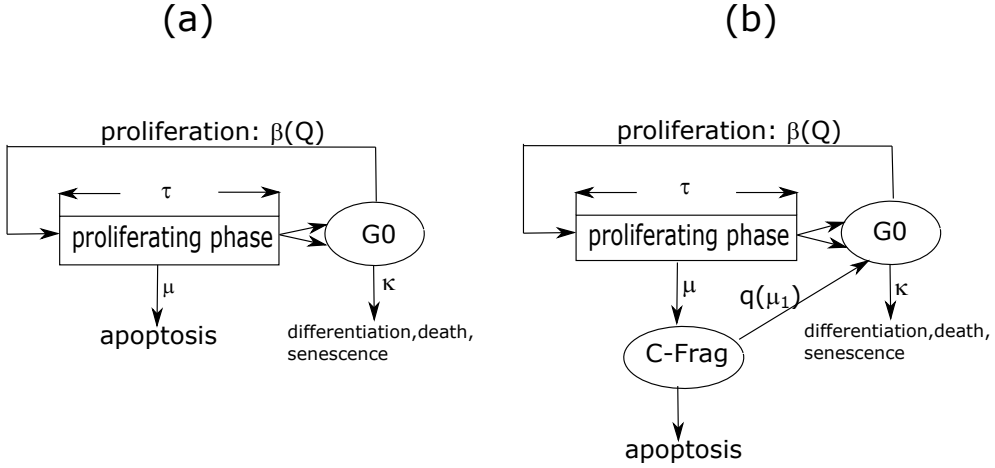

Figure 1. The G0 cell cycle model of leukemia stem cell regeneration. (a) Leukemia stem cell regeneration without chemotherapy. All stem cells are classified into the resting and the proliferative phase. During stem cell regeneration, resting phase cells either enter the proliferating phase with a rate β, or be removed from the resting pool with a rate κ due to differentiation, senescence, or death. The proliferating cells undergo apoptosis with a rate μ. At the end of the resting phase, each cell divides into two daughter cells through mitosis. (b) Leukemia stem cell regeneration under chemotherapy. Chemotherapy agents interfere the process of cell division and promote apoptosis [49]. During apoptosis, after the early stage of chromosome fragmentation, some cells survive from crisis (with a probability $q(\mu_1)$) through chromosome recombination, and the survived cells re-enter the G0 phase. Here the extra apoptosis rate μ_1 is a parameter associated with the chemotherapy dose.

The proliferation rate β is a function of the resting phase cell number Q, indicating the regulation of cell proliferation through cytokines secreted from all stem cells. Normally, the proliferation rate is a decrease function of the cell number, and approaches 0 when the cell number Q is large enough [50]. Nevertheless, in the situation of cancer, the function can be non-monotonic because cancer cells can evade growth suppressors, and produce self-sustaining proliferative signaling [51].

Now, we consider the effects of chemotherapy, which often promote cell death during the proliferative phrase due to the toxicity [49]. Hence, we write the apoptosis rate as $\mu = \mu_0 + \mu_1$, where μ_0 represents the baseline apoptosis rate in the absence of chemotherapy, and μ_1 the extra apoptosis rate due to treatment stress (the rate μ_1 is often increase with the chemotherapy dose, hence we also refer μ_1 as the dose for short). At the early apoptosis stage, the cells undergo chromosome fragmentation (C-Frag) (cell number given by $(1 - e^{-\mu\tau})\beta(Q_\tau)Q_\tau$). However, in a small population of cells with C-Frag, the fragments can rejoin to yield chromosome recombination and the cells survive from crisis and re-enter the G0 phase; other cells continue the apoptosis process (Figure. 1(b)). We

assume that the probability of chromosome recombination, $q(\mu_1)$ $(0 \le q(\mu_1) < 1)$, is dependent on the chemotherapy dose, so that $q(\mu_1)$ is an increase function. Therefore, we modify the above G0 cell cycle model (2.1) to include chromosome recombination, the cell number Q satisfies the following delay differential equation:

$$\frac{dQ}{dt} = -(\beta(Q) + \kappa)Q + (2e^{-\mu\tau} + (1 - e^{-\mu\tau})q(\mu_1))\beta(Q_\tau)Q_\tau, \tag{2.2}$$

where

$$\mu = \mu_0 + \mu_1. \tag{2.3}$$

Hereafter, we always assume that $\beta(Q)$ is a decrease function, and $q(\mu_1)$ is an increase function.

For model simulation, we refer the classical models for hematopoietic stem cells (Table 1), and take the proliferation rate $\beta(Q)$ and the probability of chromosome recombination $q(\mu_1)$ as Hill type functions [44, 50]:

$$\beta(Q) = \beta_0 \frac{\theta^n}{\theta^n + Q^n} + \beta_1, \quad q(\mu_1) = q_1 \frac{\mu_1^m}{e^m + \mu_1^m}. \tag{2.4}$$

Table 1. Default parameter values. The parameter values for hematopoietic stem cells are referred to [44, 50, 52], and β_1 is set to 0 for default, other parameters for the chemotherapy effect are taken arbitrary.

Parameter	Value	Unit	Source
Q^*	1.53	$\times 10^6$ cells/kg	[44, 52]
β_0	8.0	day^{-1}	[44, 50]
β_1	0	day^{-1}	-
θ	0.096	$\times 10^6$ cells/kg	[44, 50]
n	2	-	[44]
q_1	1	day^{-1}	-
e	0.34	day^{-1}	-
m	4	-	-
κ	0.02	day^{-1}	[44, 50]
τ	2.8	days	[44, 52]
μ_0	0.001	day^{-1}	[44, 50]

3. Results

3.1. Dependence of the steady state with drug dosage

From (2.2), the steady state $Q(t) \equiv Q^*$ is given by the equation

$$-(\beta(Q^*) + \kappa)Q^* + (2e^{-\mu\tau} + (1 - e^{-\mu\tau})q(\mu_1))\beta(Q^*)Q^* = 0.$$

Obviously, there is a zero solution $Q^* = 0$. When the proliferation rate $\beta(Q)$ is a decrease function, there is a positive steady state $Q^* > 0$ if and only if the condition

$$\beta_0 > \frac{\kappa}{2e^{-\mu\tau} - 1 + (1 - e^{-\mu\tau})q(\mu_1)} - \beta_1 > 0 \tag{3.1}$$

is satisfied, and the steady state is given by the root of

$$\beta(Q^*) = \frac{\kappa}{2e^{-\mu\tau} - 1 + (1 - e^{-\mu\tau})q(\mu_1)}. \tag{3.2}$$

From (3.1), there exists a positive steady state when the recombination rate $q(\mu_1)$ satisfies

$$\frac{\kappa}{(\beta_0 + \beta_1)(1 - e^{-\mu\tau})} < q(\mu_1) + \frac{2e^{-\mu\tau} - 1}{1 - e^{-\mu\tau}} < \frac{\kappa}{\beta_1(1 - e^{-\mu\tau})}. \tag{3.3}$$

Specifically, if

$$q(\mu_1) + \frac{2e^{-\mu\tau} - 1}{1 - e^{-\mu\tau}} < \frac{\kappa}{(\beta_0 + \beta_1)(1 - e^{-\mu\tau})}, \tag{3.4}$$

the system has only zero solution steady state, and the zero solution is global stable which means the situation of no cells; and if

$$q(\mu_1) + \frac{2e^{-\mu\tau} - 1}{1 - e^{-\mu\tau}} > \frac{\kappa}{\beta_1(1 - e^{-\mu\tau})}, \tag{3.5}$$

the zero solution is unstable and all positive solutions approach to $+\infty$, which means the situation of uncontrolled cell growth.

Next, we consider the stability of the steady states. Let $x(t) = Q(t) - Q^*$ and linearize the equation (2.2) at $x = 0$, we obtain

$$\frac{dx}{dt} = -ax + bx_\tau, \tag{3.6}$$

where

$$\begin{aligned} a &= \beta(Q^*) + \kappa + \beta'(Q^*)Q^*, \\ b &= [2e^{-\mu\tau} + (1 - e^{-\mu\tau})q(\mu_1)][\beta(Q^*) + \beta'(Q^*)Q^*]. \end{aligned}$$

The zero solution of equation (3.6) is stable if and only if the coefficients a and b take values from the region S defined as

$$S = \{(a, b) \in \mathbb{R}^2 | a \sec \omega\tau < b < a, \text{where } \omega = -a \tan \omega\tau, a > -\frac{1}{\tau}, \omega \in (0, \frac{\pi}{\tau})\}. \tag{3.7}$$

For the zero solution $Q(t) \equiv Q^* = 0$, we have

$$a = \beta_0 + \kappa > 0,\ b = (2e^{-\mu\tau} + (1 - e^{-\mu\tau})q(\mu_1))\beta_0 > 0.$$

Hence, the zero solution is stable if and only if $b < a$, *i.e.*, the inequality (3.4) is satisfied.

For the positive steady state $Q(t) = Q^* > 0$, we have

$$a = \bar{\beta} + \kappa - \hat{\beta},\ b = (2e^{-\mu\tau} + (1 - e^{-\mu\tau})q(\mu_1))\ (\bar{\beta} - \hat{\beta}), \tag{3.8}$$

where $\bar{\beta} = \beta(Q^*) > 0$ and $\hat{\beta} = -\beta'(Q^*)Q^* > 0$. Hence, when the condition (3.1) is satisfied, the equation (3.7) gives the Hopf bifurcation curve for the positive steady state

$$\begin{cases} \hat{\beta}_{\text{crit}} &= -\dfrac{[2e^{-\mu\tau} + (1-e^{-\mu\tau})q(\mu_1)](\sec\omega\tau - 1)}{2e^{-\mu\tau} - \sec\omega\tau + (1-e^{-\mu\tau})q(\mu_1)}\bar{\beta}, \\ \omega &= -\bar{\beta}\dfrac{[2e^{-\mu\tau} + (1-e^{-\mu\tau})q(\mu_1)][2e^{-\mu\tau} - 1 + (1-e^{-\mu\tau})q(\mu_1)]}{2e^{-\mu\tau} - \sec\omega\tau + (1-e^{-\mu\tau})q(\mu_1)}\tan\omega\tau, \end{cases} \tag{3.9}$$

where ω can be solved from the second equation of (3.9), and

$$\omega \in \left[\frac{1}{\tau}\arccos\frac{1}{2e^{-\mu\tau} + (1-e^{-\mu\tau})q(\mu_1)}, \frac{\pi}{\tau}\right]. \tag{3.10}$$

When $\hat{\beta} < \hat{\beta}_{\text{crit}}$, the positive steady state solution of equation (2.2) is stable, and when $\hat{\beta} > \hat{\beta}_{\text{crit}}$, the steady state becomes unstable. Biologically, the Hopf bifurcation curve (3.9) gives the critical proliferation rate $\hat{\beta}_{\text{crit}}$, so that the steady state is stable when the proliferation rate is less than the critical rate, but when the proliferation rate is larger than the critical rate, the steady state becomes unstable and the system exhibits oscillatory dynamics, which can be a source of dynamical blood diseases [42].

In summary, we have the following conclusion:

Theorem 1. *Consider the model equation* (2.2)*, where* $\beta(Q)$ $(\beta_0 > \beta(Q) > \beta_1)$ *is a decrease function, and* $0 \le q(\mu_1) < 1$*. The equation always has zero steady state* $Q(t) \equiv 0$*; if and only if the condition*

$$\beta_0 > \frac{\kappa}{2e^{-\mu\tau} - 1 + (1-e^{-\mu\tau})q(\mu_1))} - \beta_1 > 0 \tag{3.11}$$

is satisfied, equation (2.2) *has a unique positive steady state solution* $Q(t) = Q^*$*, which is given by*

$$\beta(Q^*) = \frac{\kappa}{2e^{-\mu\tau} - 1 + (1-e^{-\mu\tau})q(\mu_1))}. \tag{3.12}$$

Moreover,

(1) the zero steady state is stable if and only if

$$q(\mu_1) + \frac{2e^{-\mu\tau} - 1}{1-e^{-\mu\tau}} < \frac{\kappa}{(\beta_0+\beta_1)(1-e^{-\mu\tau})}; \tag{3.13}$$

(2) when (3.11) *is satisfied and let* $\bar{\beta} = \beta(Q^*)$*,* $\hat{\beta} = -\beta'(Q^*)Q^*$*, for any* $\mu_1 > 0$*, there is a critical proliferation rate* $\hat{\beta}_{\text{crit}} > 0$*, defined by* (3.9)*, so that the positive steady state is stable if and only if* $\hat{\beta} < \hat{\beta}_{\text{crit}}$.

When the functions $\beta(Q)$ and $q(\mu_1)$ are defined by (2.4), equation (3.2) gives

$$\bar{\beta} = \frac{\kappa}{f}, \quad f = 2e^{-\mu\tau} - 1 + (1-e^{-\mu\tau})q(\mu_1), \tag{3.14}$$

and

$$\hat{\beta} = -\beta'(Q^*)Q^* = n(\bar{\beta} - \beta_1)(1 - \frac{\bar{\beta} - \beta_1}{\beta_0}). \tag{3.15}$$

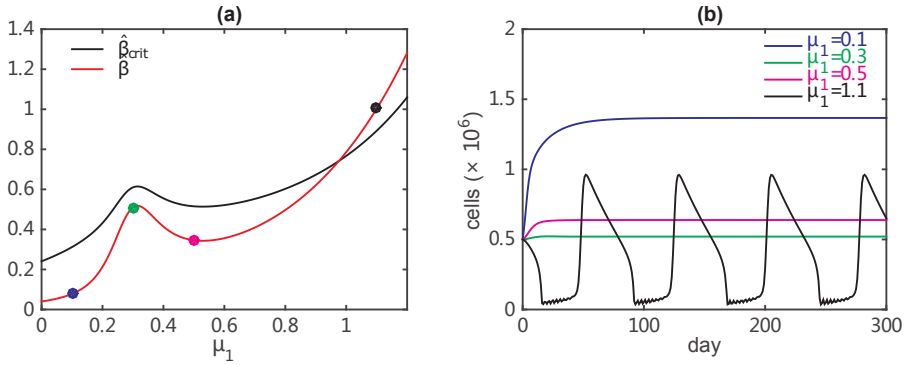

Figure 2. Bifurcation analysis of the model system. (a) Dependence of the bifurcation curve $\hat{\beta}_{\text{crit}}$ (black line) in equation (3.9) and $\hat{\beta}$ (red line) in equation (3.15) on the parameter μ_1. (b) Sample dynamics of cell population. Different color lines are obtained from different μ_1 values (same color dots in (a)): $\mu_1 = 0.1$(blue line), $\mu_1 = 0.3$(green line), $\mu_1 = 0.5$(magenta line), and $\mu_1 = 1.1$(black line). Other values are the same as default values in Table 1. In simulations, we first set the parameters as their default values, $Q(t) \equiv 0.5$ for $t < 0$, and solve the equation to $t = 300$ day.

Applying the default parameter values in Table 1, when μ_1 varies from 0 to 1.2, the critical proliferation rate $\hat{\beta}_{\text{crit}}$ (black line, given by (3.9)) and proliferation rate at the steady state $\hat{\beta}$ (red line, given by (3.15)) are shown in Figure 2(a). Here, $\hat{\beta} > \hat{\beta}_{\text{crit}}$ implies the parameter region with unstable steady state, and there are oscillatory solutions due to Hopf bifurcation (Figure 2(b)).

From Figure 2(a), when the drug dose is low, we have $\hat{\beta} < \hat{\beta}_{\text{crit}}$, and (2.2) has a stable positive steady state (Figure 2(b), blue line). The steady state cell number depends on the dose μ_1, and reach a local minimum when μ_1 takes intermediate values (green dot in Figure 2(a), also referred to Figure 3). When the drug dose further increase to a high level (black dot), the steady state of (2.2) becomes unstable, and the cell populations show oscillatory dynamics (Figure 2(b), black line).

3.2. Optimal dose of chemotherapy

From the above analyses, when

$$f = 2e^{-\mu\tau} - 1 + (1 - e^{-\mu\tau})q(\mu_1) > 0,\ \beta_1 < \frac{\kappa}{f} < \beta_0 + \beta_1, \tag{3.16}$$

the equation (2.2) has a unique positive steady state $Q(t) = Q^*$. Moreover, let $\bar{\beta} = \beta(Q^*)$, then $\bar{\beta} = \kappa/f$, and

$$0 < \bar{\beta} - \beta_1 < \beta_0.$$

Hence, the steady state can be expressed explicitly as

$$Q^* = \theta \sqrt[n]{\frac{\beta_0}{\bar{\beta} - \beta_1} - 1}. \tag{3.17}$$

Equation (3.17) shows that the steady state Q^* is dependent on the chemotherapy dose parameter μ_1 through $\bar{\beta} = \kappa/f$. The following theorem shows that under certain conditions, there is an optimal dose (within a tolerated dose) so that the steady state cell number reach a local minimum.

Theorem 2. *Consider the equation* (2.2)*, if the following conditions are satisfied*

(1) the functions $\beta(Q)$ *and* $q(\mu_1)$ *are continuous, and satisfy*

$$\beta_0 + \beta_1 > \beta(Q) > \beta_1 \geq 0,\ 1 \geq q(\mu_1) \geq 0,\ \beta'(Q) < 0,\ q'(\mu_1) > 0,$$

(2) the parameters $(\beta_0, \beta_1, \kappa, \mu_0,$ *and* $\tau)$ *satisfy the condition* (3.16) *(here we note* $\mu = \mu_0 + \mu_1$*),*
(3) both $q(0)$ *and* $q'(0)$ *are sufficiently small,*
(4) there exists $\mu_1^* > 0$ *so that conditions (1)-(2) are satisfied when* $\mu_1 \in (0, \mu_1^*)$*, and*

$$q(\mu_1^*) + q'(\mu_1^*)\tau^{-1}(e^{(\mu_0+\mu_1^*)\tau} - 1) > 2,$$

the steady state Q^* *reaches a local minimum value at an optimal dose* $\mu_1 = \hat{\mu}_1 \in (0, \mu_1^*)$*.*

Proof. When the conditions (1) and (2) are satisfied, equation (2.2) has a unique positive steady state $Q(t) \equiv Q^*$, which is given by (3.17). Hence, we have

$$\begin{aligned}
\frac{dQ^*}{d\mu_1} &= \frac{\theta}{n}\left(\frac{\beta_0}{\bar{\beta} - \beta_1} - 1\right)^{\frac{1}{n}-1} \frac{-\beta_0}{(\bar{\beta} - \beta_1)^2} \frac{d\bar{\beta}}{d\mu_1} \\
&= \frac{\theta}{n}\left(\frac{\beta_0}{\bar{\beta} - \beta_1} - 1\right)^{\frac{1}{n}-1} \frac{-\beta_0}{(\bar{\beta} - \beta_1)^2} \frac{-\kappa}{f^2} \frac{df}{d\mu_1} \\
&= \frac{\theta}{n}\left(\frac{\beta_0}{\bar{\beta} - \beta_1} - 1\right)^{\frac{1}{n}-1} \frac{\beta_0\kappa}{(\bar{\beta} - \beta_1)^2 f^2} \frac{df}{d\mu_1},
\end{aligned}$$

and

$$\frac{df}{d\mu_1} = \tau e^{-\mu\tau}(q(\mu_1) + q'(\mu_1)\tau^{-1}(e^{\mu\tau} - 1) - 2). \tag{3.18}$$

Hence, the sign of $\dfrac{dQ^*}{d\mu_1}$ is determined by the sign of $\dfrac{df}{d\mu_1}$.

The condition (3) implies $\left.\dfrac{df}{d\mu_1}\right|_{\mu_1=0} < 0$, and condition (4) implies $\left.\dfrac{df}{d\mu_1}\right|_{\mu_1=\mu_1^*} > 0$. Hence, there exists an optimal value $\hat{\mu}_1 \in (0, \mu_1^*)$, so that $\left.\dfrac{dQ^*}{d\mu_1}\right|_{\mu_1=\hat{\mu}_1} = 0$, thus Q^* reaches a local minimum value at $\mu_1 = \hat{\mu}_1$. □

Figure 3 shows the dependence of steady state with the dose μ_1 when we take parameters from Table 1, which exhibits a local minimum at about $\hat{\mu}_1 = 0.3$. Here we note that the steady state cell number Q^* decrease with further increasing of $\mu_1 > 0.5$ and approaches zero when μ_1 is large enough. However, clinically, higher level μ_1 may exceed the maximum tolerated dose, and have a risk to induce oscillatory dynamics (Figure 2, and the discussion below). Hence, there is an optimal dose within a certain region (for example, $\mu_1 < 0.5$) so that the cell number reaches a relative low level.

3.3. Chemotherapy-induced oscillations

Above analyses show that chemotherapy may induce oscillatory dynamics through Hopf bifurcation when μ_1 takes proper values. Here, we further analyze the condition for Hopf bifurcation, and identify how clinical conditions may affect the chemotherapy-induced oscillations [46].

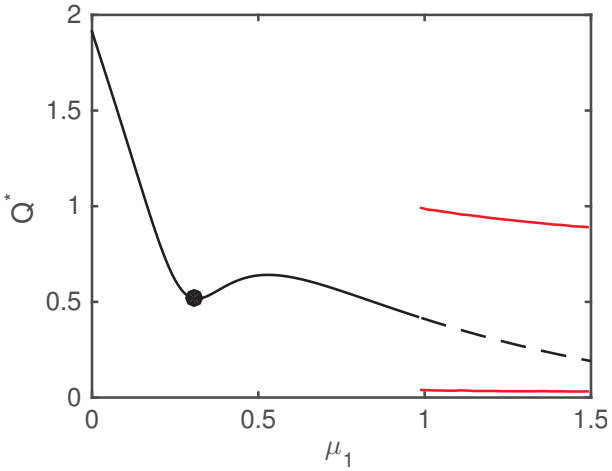

Figure 3. Dependence of the steady state Q^* with chemotherapy dose μ_1. Black lines show the steady state, with solid line for the stable steady state, and dashed line for the unstable steady state. Red lines show the upper and lower bounds of the oscillation solutions when the steady state is unstable.

Hematopoiesis can exhibit oscillations in one or several circulating cell types and show symptoms of periodic hematological diseases [43, 53]. Here, we show the conditions to induce oscillations, and try to identify the criteria to avoid therapy-induced oscillations in cancer treatments.

Using the previously introduced notations $\bar{\beta}$ and f in (3.14), the bifurcation curve (3.9) can be rewritten as

$$\begin{cases} \hat{\beta}_{\text{crit}} &= -\dfrac{(f+1)(\sec\omega\tau - 1)}{f+1-\sec\omega\tau}\bar{\beta}, \\ \omega &= -\bar{\beta}\dfrac{f(f+1)\tan\omega\tau}{f+1-\sec\omega\tau}, \end{cases} \tag{3.19}$$

and hence

$$\hat{\beta}_{\text{crit}} = \omega\frac{1-\cos\omega\tau}{f\sin\omega\tau}. \tag{3.20}$$

Moreover, from equation (3.15), we have

$$\bar{\beta} = \frac{\kappa}{f}, \quad \hat{\beta} = -\beta'(Q^*)Q^* = n(\frac{\kappa}{f} - \beta_1)(1 - \frac{\kappa/f - \beta_1}{\beta_0}). \tag{3.21}$$

Hence, from (3.19)–(3.21), and the bifurcation condition $\hat{\beta}_{\text{crit}} = \hat{\beta}$, we obtain the bifurcation curve in terms of f and κ (defined by a parameter $\omega > 0$) as

$$\begin{cases} \omega\dfrac{1-\cos\omega\tau}{f\sin\omega\tau} &= n(\dfrac{\kappa}{f} - \beta_1)(1 - \dfrac{\kappa/f - \beta_1}{\beta_0}), \\ \omega &= -\dfrac{\kappa(f+1)\tan\omega\tau}{f+1-\sec\omega\tau}. \end{cases} \tag{3.22}$$

Thus, given the parameter $\beta_0, \beta_1, n, \tau$, equation (3.22) defines a bifurcation curve in the κ-f plane when ω varies over the region in (3.10).

Figure 4 shows the bifurcation curves obtained from (3.22). For any $\kappa > 0$, there exist an upper bound $\overline{f}$ and a lower bound $\underline{f}$, so that the positive steady state (if exists) is stable when $\underline{f} < f < \overline{f}$.

Moreover, when the self-sustained proliferation rate β_1 increases, the lower bound $\underline{f}$ is independent of β_1, while the upper bound $\overline{f}$ decreases with β_1. Here, we note that f depends on the dose parameter μ_1 through (3.14), these results provide a strategy to quantitatively control the chemotherapy dose to avoid therapy-induced oscillation, *i.e.*, try to take values from the gray region for different differentiation rate κ.

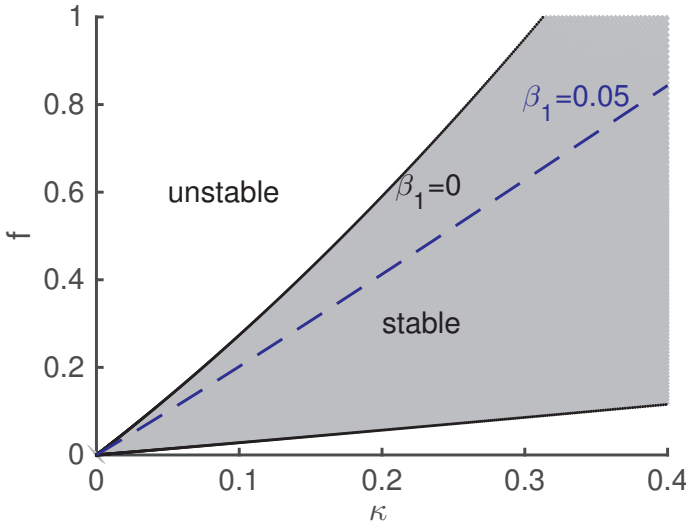

Figure 4. Hopf bifurcation curve in the κ-f plane. The black solid lines are obtained from (3.22) with $\beta_0 = 0$, the blue dashed line is obtained from (3.22) with $\beta_1 = 0.05$. Gray shadow shows the parameter region of stable steady state.

4. Discussion

The era of chemotherapy has been ruled by the routine use of dose-intense protocols based on the "maximum-tolerate dose" concept. This protocol plays a prominent role in veterinary oncology, however there are many debates on using the high dose chemotherapy because of the side effects and recurrence rates [54]. Chromosome recombination induced by chemotherapy is a source to produce chaotic genome in cancer cells and may lead to drug resistance. Here, we present a mathematical model to consider cell population dynamics in response to chemotherapy with occasional occurrence of chromosome recombination. Model analyses show that maximum-tolerate dose may not always result in the best outcome when the probability of chromosome recombination is dependent on the dose; there is an optimal dose within a tolerated dose so that the steady state tumor cell number reaches a relative low level. Moreover, sustained administration of high dose chemotherapy may induced oscillatory cell population dynamics through Hopf bifurcation. Clinically, the long period oscillation can be considered as the frequent recurrence of tumor cells, which is a result of drug-resistant or chemotherapy-induced dynamical disease. For instance, the periodic chronic myelogenous leukemia show obvious oscillations in circulating blood cells [55]. We identify the parameter regions for the occurrence of oscillation dynamics, which is valuable when we try to avoid the frequent recurrence. To our knowledge, this is the first try to quantitatively study the tumor cell population dynamics in response to chemotherapy when chromosome recombination is induced. Genome chaotic has been

widely reported in studies of genomic structure of cancer cells, however how genome chaotic play roles in cancer development and drug resistance is not well documented. The current study is the first try to consider this issue. Here, the proposed model only consider the main effect of cell survival from C-Frag through chromosome recombination. Nevertheless, many other effects should be included for a complete understanding of drug resistance due to the chromosome changes induced by cancer therapy. Moreover, the cell heterogeneity can also play important roles in drug resistance. These effects should be extended to the current model in order to obtain an optimal dose of chemotherapy.

Acknowledgments

This work was supported by grant from National Natural Science Foundation of China (91730301, 11762011).

Conflict of interest

No potential conflicts of interest were disclosed.

References

1. N. Beerenwinkel, C. D. Greenman, and J. Lagergren, Computational Cancer Biology: An Evolutionary Perspectiv, *PLoS Comput. Biol.*, **12** (2016), e1004717.
2. N. Beerenwinkel, R. F. Schwarz, M. Gerstung, et al., Cancer evolution: Mathematical models and computational inference, *Syst. Biol.*, **64** (2015), e1–e25.
3. S. Blum, F. Martins and M. Lübbert, Immunotherapy in adult acute leukemia, *Leuk. Res.*, **60** (2017), 63–73.
4. C. H. June, R. S. O'Connor, O. U. Kawalekar, et al., CAR T cell immunotherapy for human cancer, *Science*, **359** (2018), 1361–1365.
5. L. Labanieh, R. G. Majzner and C. L. Mackall, Programming CAR-T cells to kill cancer, *Nat. Biomed. Eng.*, **2** (2018), 377–391.
6. M. H. Abdul-Aziz, J. Lipman, J. W. Mouton, et al., Applying pharmacokinetic/pharmacodynamic principles in critically ill patients: Optimizing efficacy and reducing resistance development, *Semin. Respir. Crit. Care Med.*, **36** (2015), 136–153.
7. W. J. Aston, D. E. Hope, A. K. Nowak, et al., A systematic investigation of the maximum tolerated dose of cytotoxic chemotherapy with and without supportive care in mice, *BMC Cancer*, **17** (2017), 684.
8. C. Hudis and C. Danq, The development of dose-dense adjuvant chemotherapy, *Breast J.*, **21** (2015), 42–51.
9. A. Matikas, T. Foukakis and J. Berqh, Dose intense, dose dense and tailored dose adjuvant chemotherapy for early breast cancer: An evolution of concepts, *Acta Oncol.*, **56** (2017), 1143–1151.
10. T. Prasanna, J. Beith, S. Kao, et al., Dose modifications in adjuvant chemotherapy for solid organ malignancies: A systematic review of clinical trials, *Asia Pac. J. Clin. Oncol.*, **14** (2018), 125–133.

11. J. A. Roberts, P. Kruger, D. L. Paterson, et al., Antibiotic resistance: What's dosing got to do with it? *Crit. Care Med.*, **36** (2008), 2433–2440.

12. C. L. Tourneau, J. J. Lee and L. L. Siu, Dose escalation methods in phase I cancer clinical trials, *J. Natl. Cancer Inst.*, **101** (2009), 708–720.

13. J. Y. Lin, H. M. He, Y. Yang, et al., Comparison of two different treatment regimens for curative effect and recurrence rate in patients with extranodal nasal type NK/T cell lymphoma, *Chin. J. Clin. Res.*, **29** (2016), 1042–1045.

14. Y. Yang, Y. Wen, C. Bedi, et al., The relationship between cancer patient's fear of recurrence and chemotherapy: A systematic review and meta-analysis, *J. Psychosomatic Res.*, **98** (2017), 55–63.

15. Y. A. Luqmani, Mechanisms of drug resistance in cancer chemotherapy, *Med. Princ. Pract.*, **14** (2005), 35–48.

16. M. Moschovi, E. Critselis, O. Cen, et al., Drugs acting on homeostasis: Challenging cancer cell adaptation, *Expert Rev. Anticancer Ther.*, **15** (2015), 1405–1417.

17. J. Zhang, J. J. Cunningham, J. S. Brown, et al., Integrating evolutionary dynamics into treatment of metastatic castrate-resistant prostate cancer, *Nat. Commun.*, **8** (2017), 1816.

18. H. Easwaran, H. C. Tsai and S. B. Baylin, Cancer epigenetics: Tumor heterogeneity, plasticity of stem-like states, and drug resistance, *Mol. Cell*, **54** (2014), 716–727.

19. C. E. Meacham and S. J. Morrison, Tumour heterogeneity and cancer cell plasticity, *Nature*, **501** (2013), 328–337.

20. C. Kim, R. Gao, E. Sei, et al., Chemoresistance evolution in triple-negative breast cancer delineated by single-cell sequencing, *Cell*, **173** (2018), 879–893.

21. Y. Su, W. Wei, L. Robert, et al., Single-cell analysis resolves the cell state transition and signaling dynamics associated with melanoma drug-induced resistance, *Proc. Natl. Acad. Sci. USA*, **114** (2017), 13679–13684.

22. H. Sakahira, M. Enari and S. Nagata, Cleavage of CAD inhibitor in CAD activation and DNA degradation during apoptosis, *Nature*, **391** (1998), 96–99.

23. G. Liu, J. B. Stevens, S. D. Horne, et al., Genome chaos: Survival strategy during crisis, *Cell Cycle*, **13** (2014), 528–537.

24. J. B. Stevens, B. Y. Abdallah, G. Liu, et al., Diverse system stresses: Common mechanisms of chromosome fragmentation, *Cell Death Dis.*, **2** (2011), e178.

25. C. Gao, Y. Su, J. Koeman, et al., Chromosome instability drives phenotypic switching to metastasis *Proc. Natl. Acad. Sci. USA*, **113** (2016), 14793–14798.

26. H. H. Heng and J. B. Stevens, Patterns of genome of dynamics and cancer evolution, *Cell. Oncol.*, **30** (2008), 513–514.

27. J. B. Stevens, S. D. Horne, B. Y. Abdallah, et al., Chromosomal instability and transcriptome dynamics in cancer, *Cancer Metastasis Rev.*, **32** (2013), 391–402.

28. J. B. Stevens, G. Liu, B. Y. Abdallah, et al., Unstable genomes elevate transcriptome dynamics, *Int J. Cancer*, **134** (2014), 2074–2087.

29. P. M. Altrock, L. L. Liu and F. Michor, The mathematics of cancer: Integrating quantitative models, *Nat. Rev. Cancer*, **15** (2015), 730–745.

30. F. S. Borges, K. C. Iarosz, H. P. Ren, et al., Model for tumour growth with treatment by continuous and pulsed chemotherapy, *BioSystems*, **116** (2014), 43–48.

31. H. Cho and D. Levy, Modeling the dynamics of heterogeneity of solid tumors in response to chemotherapy, *Bull. Math. Biol.*, **79** (2017), 2986–3012.

32. K. C. Larosz, F. S. Borges, A. M. Batista, et al., Mathematical model of brain tumour with glia-neuron interactions and chemotherapy treatment, *J. Theor. Biol.*, **368** (2015), 113–121.

33. Á.G. López, K.C. Larosz, A.M. Batista, et al., Nonlinear cancer chemotherapy: Modelling the Norton-Simon hypothesis, *Commun. Nonlinear Sci. Numer Simul.*, **70** (2019), 307–317.

34. F. Michor, Mathematical models of cancer stem cells, *J. Clin. Oncol.*, **26** (2008), 2854–2861.

35. H. H. Heng, S. M. Regan, G. Liu, et al., Why it is crucial to analyze non clonal chromosome aberrations of NCCAs? *Mol. Cytogenet.*, **9** (2016), 15.

36. C. Colijin and M. C. Mackey, A mathematical model of hematopoiesis: I. Periodic chronic myelogenous leukemia, *J. Theor. Biol*, **237** (2005), 117–132.

37. C. Colijin and M. C. Mackey, A mathematical model of hematopoiesis: II. Cyclical neutropenia, *J. Theor. Biol.*, **237** (2005), 133–146.

38. A. C. Fowler and M. C. Mackey, Relaxation oscillations in a class of delay differential equations, *SIAM J. Appl. Math.*, **63** (2002), 299–323.

39. L. Pujo-Menjouet, S. Bernard and M. C. Mackey, Long period oscillations in a model of hematopoietic stem cells, *SIAM J. Appl. Dyn. Syst.*, **4** (2005), 312–332.

40. F. Burns and I. Tannock, On the existence of a G_0 phase in the cell cycle, *Cell Tissue Kinet.*, **3** (1970), 321–334.

41. M. C. Mackey and P. Dormer, Continuous maturation of proliferating erythroid precursor, *Cell Tissue Kinet.*, **15** (1982), 381–392.

42. M. C. Mackey and J. G. Milto, Dynamical disease, *Ann. New York Acad. Sci.*, **504** (1987), 16–32.

43. D. C. Dale and M. C. Mackey, Understanding, treating and avoiding hematological disease: Better medicine through mathematics? *Bull. Math. Biol.*, **77** (2015), 739–757.

44. J. Lei and M. C. Mackey, Multisability in an age-structured model of hematopoiesis: Cyclical neutropenia, *J. Theor. Biol.*, **270** (2011), 143–153.

45. M. C. Mackey, Cell kinetic status of haematopoietic stem cells, *Cell Prolif.*, **34** (2001), 71–83.

46. C. Zhuge, M. C. Mackey and J. Lei, Origins of oscillation patterns in cyclical thrombocytopenia, *J. Theor. Biol.*, **462** (2019), 432–445.

47. G. Brooks, G. Provencher, J. Lei, et al., Neutrophil dynamics after chemotherapy and G-CSF: The role of pharmacokinetics in shaping the response, *J. Theor. Biol.*, **315** (2012), 97–109.

48. C. Zhuge, J. Lei and M. C. Mackey, Neutrophil dynamics in response to chemotherapy and G-CSF, *J. Theor. Biol.*, **293** (2012), 111–120.

49. Y. Hannun, Apoptosis and dilemma of cancer chemotherapy, *Blood*, **89** (1997), 1845–1853.

50. S. Bernard, J. Belair and M. C. Mackey, Oscillations in cyclical neutropenia: New evidence based in mathematical modeling, *J. Theor. Biol.*, **223** (2003), 283–298.

51. D. Hanahan and R.A. Weinberg, Hallmarks of cancer: The next generation, *Cell*, **144** (2011), 646–674.

52. J. Abkowitz, R. Holly and W. P. Hammond, Cyclic hematopoiesis in dogs: Studies of erythroid burst forming cells confirm and early stem cell defect, *Exp. Hematol.*, **16** (1988), 941–945.

53. C. Foley and M. C. Mackey, Dynamic hematological disease: A review, *J. Math. Biol.*, **58** (2009), 285–322.

54. T. B. Gaspar, J. Henriques, L. Marconato, et al., The use of low-dose metronomic chemotherapy in dogs-insight into a modern caner field, *Vet. Comp. Oncol.*, **16** (2018), 2–11.

55. A. Safarishahribijari and A. Gaffari, Parameter identification of hematopoiesis mathematical model – periodic chronic myelogenous leukemia, *Contemp. Oncol(Pozn).*, **17** (2013), 73–77.

AIMS Press

© 2019 the Author(s), licensee AIMS Press. This is an open access article distributed under the terms of the Creative Commons Attribution License (http://creativecommons.org/licenses/by/4.0)